ELSEVIER

Journal of Molecular Catalysis A: Chemical 144 (1999) 117–122

JOURNAL OF MOLECULAR CATALYSIS A: CHEMICAL

www.elsevier.com/locate/molcata

Catalytic hydrogenation of carbon dioxide over $LaNi_5$ activated during the reaction

Hisanori Ando *, Masahiro Fujiwara, Yasuyuki Matsumura, Mutsuo Tanaka, Yoshie Souma

Osaka National Research Institute, AIST, Midorigaoka, Ikeda, Osaka 563-8577, Japan

Received 19 May 1998; accepted 13 September 1998

Abstract

The hydrogenation of carbon dioxide to methane can be catalyzed over an intermetallic compound of $LaNi_5$ at 250–350°C. The catalytic activity at 250°C increases during the reaction while X-ray diffraction (XRD) analyses show that the structure of the compound decomposes to $La(OH)_3$, $LaCO_3OH$, and metallic nickel. Formation of metallic nickel species during the reaction also takes place in a nickel–lanthanum oxides catalyst prepared by a coprecipitation method, however, the activity is not so high as the former catalyst. Surface analyses by X-ray photoelectron spectroscopy (XPS) suggest that new nickel species interacting with lanthanum cation, possibly Ni–O–La, are formed in $LaNi_5$ during the reaction, and the species are supposed to be rather active than metallic nickel.

Keywords: Carbon dioxide; Hydrogenation; Methane; Nickel catalyst; Intermetallic compound; XPS

1. Introduction

Many of hydrogen storage alloys are intermetallic compounds composed of rare earth metals and transition metals [1]. Their catalytic properties especially for hydrogenation have been extensively investigated because they can store hydrogen as metal hydride which is often active to the hydrogenation of olefins at temperatures lower than 40°C [2–6]. The alloys can also be applied for the hydrogenation of carbon oxides above 100°C [7–13]. The catalytic activities of the nickel-based alloys are generally high while under the reaction conditions, the structure of the intermetallic compound is changed and the growth of the transition metal particles can be observed.

The catalytic activity of nickel to the hydrogenation of carbon dioxide is known very well [14,15]. Addition of rare earth elements to nickel catalysts often results in the enhancement of the activity to the hydrogenation of carbon oxides [12,16–18]. In the case of lanthanum cobalt intermetallic catalysts, it was shown that the strong interaction between cobalt and the rare earth causes formation of new active sites [19]. This suggests that interaction between nickel and rare earth elements is important and hydrogen storage alloys are rather good precursors.

* Corresponding author. Tel.: +81-727-51-9652; Fax: +81-727-51-9629; E-mail: h-ando@onri.go.jp

1381-1169/99/$ - see front matter
PII: S1381-1169(98)00339-2

However, it is not obvious how the rare earth elements affect the catalytic activity and the further understanding is necessary for the development of the hydrogenation catalysts prepared from hydrogen storage alloys.

In this paper, we will show that the interaction between nickel and lanthanum affects the activity of the catalyst whose precursor is an intermetallic compound of $LaNi_5$ for the hydrogenation of carbon dioxide.

2. Experimental

2.1. Catalyst preparation

An intermetallic compound, $LaNi_5$, was prepared by arc-melting of the metal constituents in a copper crucible under 66.7 kPa of an argon stream. The ingot was pulverized into powder by hydrogen absorption, then the particles of 145–200 mesh were sieved for catalytic tests.

A mixed oxide of Ni and La (denoted as Ni_5LaO_x) was prepared by coprecipitation from an aqueous solution of the metal nitrates (0.83 M for Ni^{2+}, 0.17 M for La^{3+}) with a sodium carbonate solution (1 M). The precipitate was well washed with distilled water and dried at 120°C for 6 h. The solid was calcined in air at 350°C for 3 h, and crushed into 24–40 mesh granules.

Nickel powder with the particle size of ca. 210 mesh was obtained from Nihon Kagaku Sangyo.

2.2. Reaction procedure

The hydrogenation of carbon dioxide was carried out with a fixed-bed flow reactor made of stainless steel tube with 10-mm i.d. A catalyst (1.0 g) was usually pretreated with a hydrogen stream diluted with nitrogen (H_2, 1 mol%) under atmospheric pressure at 250°C for 12 h. After introduction of a reactant mixture of carbon dioxide (20 mol%) and hydrogen (80 mol%) at 250°C, the pressure was raised to 5 MPa (total flow rate, 3.0 $dm^3\ h^{-1}$ in S.T.P.). The effluent gas was analyzed with an on-line gas chromatograph whose columns were Porapak Q for carbon dioxide and MS-13X for methane and carbon monoxide. Yields and selectivities were calculated from the molar fraction of carbon in the products.

2.3. Characterization of the catalyst

X-ray diffraction (XRD) patterns were recorded with a Rigaku ROTAFLEX diffractometer (Cu-Kα). The crystallite size of the catalyst was calculated from the peak width of the XRD pattern using the equation of Scherrer [20].

Surface analyses by X-ray photoelectron spectroscopy (XPS) were performed with a Shimadzu ESCA-750. The spectra were recorded after argon-ion sputtering for 0.5 min (2 kV, 25 mA). The binding energy was corrected with the energy of C(1s) (284.6 eV) for carbon contaminant [21].

The BET surface areas of the samples were measured with a Quantasorb Jr. by the physisorption of krypton at −196°C.

3. Results

3.1. Catalytic performance of the catalysts

The hydrogenation of carbon dioxide to methane was carried out over $LaNi_5$ at 250–350°C. The conversion at 250°C increased gradually with time-on-stream and the conversion of carbon dioxide reached to ca. 94% at 5 h-on-stream and the catalytic activity became stable (Fig. 1). Trace amounts of carbon monoxide and ethane were formed as by-products, but no C_{3+} hydrocarbons were detected. The catalytic activity increased within 2 h when the reaction temperature was 350°C. After the reaction at 350°C for 10 h, the reaction temperature was reduced to 250°C. The catalytic activity was almost the same as that produced in the reaction at 250°C for 10 h without the hysteresis, that is, the

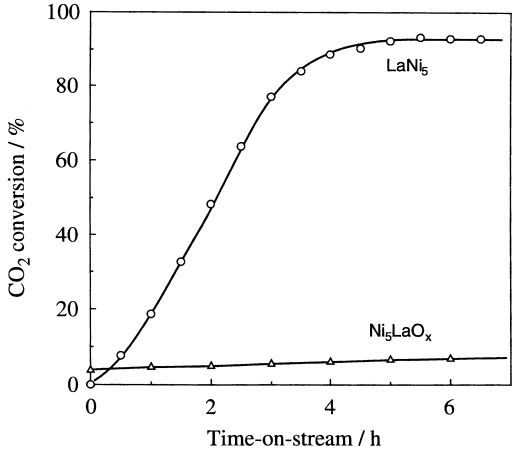

Fig. 1. Hydrogenation of carbon dioxide to methane at 250°C. (○), $LaNi_5$; (△), Ni_5LaO_x.

conversion was 92% (Table 1). The catalyst reduced at 400°C for 12 h and that without reduction produced almost the same activity as the one reduced at 250°C.

In the case of Ni_5LaO_x, the catalytic activity was increased during the reaction at 250°C for 10 h, but the conversion reached was only 8% (see Fig. 1). The CO_2 conversion at 350°C increased with in 0.5 h-on-stream and the activity was as high as that for $LaNi_5$. However, the conversion at 250°C after the reaction at 350°C for 10 h was the same as that without the reaction at 350°C (see Table 1). No change in the activity was observed over Ni powder catalyst which produced methane with the conversion of 86% at 350°C. The conversion at 250°C was significantly low as 1.1% and that was not increased after the reaction at 350°C for 10 h.

The BET surface areas were less than 0.1 $m^2 g^{-1}$ for all the samples after the reaction.

Table 1
Catalytic activities after the reaction at 350°C for 10 h

Catalyst	Temp. CO_2 (°C)	Conv. (%)	Selectivity (%)		
			CH_4	C_2H_6	CO
$LaNi_5$	250	93.6	98.1	1.9	0
	300	95.1	98.8	1.2	0
	350	95.1	100	0	0
Ni_5LaO_x	250	7.9	89.6	0	10.4
	300	54.4	95.3	2.1	2.6
	350	95.4	100	0	0
Ni powder	250	1.1	100	0	0
	300	12.4	100	0	0
	350	85.8	100	0	0

3.2. XRD analyses

XRD analyses were carried out with different aliquots of $LaNi_5$ taken out from the reactor just after the pretreatment with H_2 at 250°C for 12 h and after the reaction for 0.5–6.5 h. A typical XRD pattern of the intermetallic compound was recorded with $LaNi_5$ just after the pretreatment (Fig. 2a; solid circles) [22], but the intensity of the peaks was reduced with the time period of the reaction (Fig. 2b–d) and the clear peaks

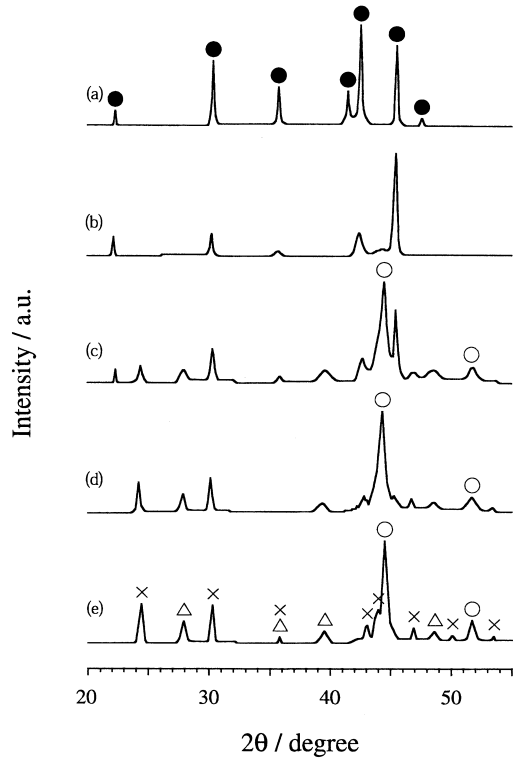

Fig. 2. X-ray diffraction (XRD) patterns for $LaNi_5$, (a) just after pretreatment, (b) after reaction at 250°C for 0.5 h, (c) 2 h, (d) 4 h, (e) 6.5 h. (●), $LaNi_5$; (○), Ni; (△), $La(OH)_3$; (×), $LaCO_3OH$.

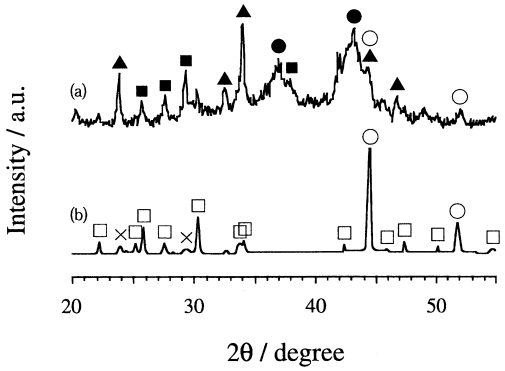

Fig. 3. XRD patterns for Ni_5LaO_x, (a) just after pretreatment, (b) after reaction at 350°C. (●), NiO; (▲), La_2NiO_4; (■), La_2O_3; (○), Ni; (□), $La_2O_2CO_3$; (×), $LaCO_3OH$.

attributed to metallic nickel ($2\theta = 44.7$ and 52.2°) appeared (Fig. 2c, d and e; open circles) [22]. The crystallite sizes of nickel in the samples after the reaction for 4–6.5 h were estimated as 11–18 nm. Lanthanum was supposed to transform into La_2O_3, however, the peaks were not found in the XRD patterns while peaks for $La(OH)_3$ (Fig. 2e; triangles) and $LaCO_3OH$ (crosses) were clearly observed [22]. No peaks attributed to nickel carbide were recorded.

Peaks attributed to NiO (Fig. 3a; solid circles) [22], La_2O_3 (solid squares) [22], and La_2NiO_4 (solid triangles) [18] were recorded in the XRD pattern of Ni_5LaO_x just after the pretreatment with hydrogen while the peaks of metallic nickel (open circles) were also observed. The peaks of the oxides disappeared and the intensity of the peaks for metallic nickel significantly increased in the pattern for the sample taken out from the reactor after the reaction at 350°C (Fig. 3b). The peaks attributed to $La_2O_2CO_3$ (squares) and $LaCO_3OH$ (crosses) were also seen in the pattern [22]. Only peaks attributed to metallic nickel were observed with Ni powder stabilized after the reaction at 350°C (not shown). The crystallite sizes of metallic nickel for Ni_5LaO_x and Ni powder after the reaction were estimated as 29 and 35 nm, respectively.

3.3. Surface analyses by XPS

In order to clarify the source of the high activity of $LaNi_5$ at 250°C, XPS analyses were performed with the catalysts after the reactions at 250°C. The spectra for Ni($2p_{3/2}$) were deconvoluted into two Gaussian peaks and the peak at 852.7–852.8 eV was attributed to metallic nickel, while the broad peak at 854.8–855.3 eV was attributed to Ni^{2+} (Fig. 4) [21]. The peak width and the intensity of the broad peak increased with an increase in the time-period of the reaction. The profiles for O(1s) were also separated into two Gaussian peaks at 531.7–

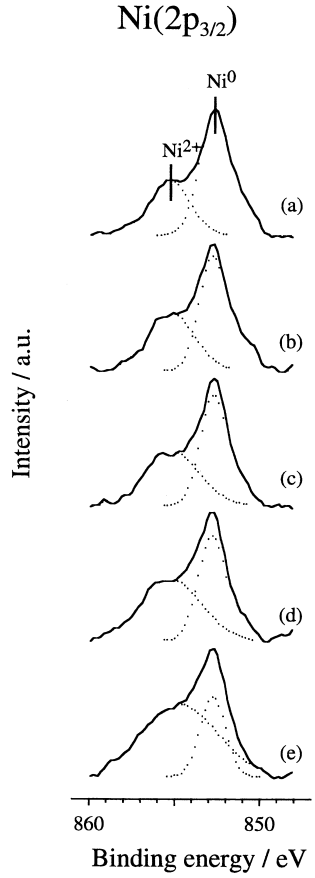

Fig. 4. X-ray photoelectron spectroscopy (XPS) spectra of Ni-($2p_{3/2}$) for $LaNi_5$, (a) just after pretreatment, (b) after reaction for 0.5 h, (c) 2 h, (d) 4 h, (e) 6.5 h.

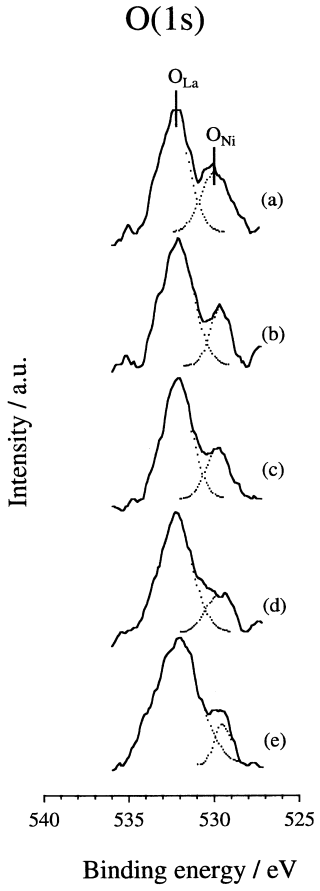

Fig. 5. XPS spectra of O(1s) for $LaNi_5$, (a) just after pretreatment, (b) after reaction for 0.5 h, (c) 2 h, (d) 4 h, (e) 6.5 h.

532.2 eV and 529.3–529.6 eV (Fig. 5). The peak position of La($3d_{5/2}$) was at 835.4 eV for the sample after the reaction for 6.5 h, while that was at 834.7 eV just after the pretreatment with hydrogen (not shown). Since the binding energy of La($3d_{5/2}$) for La_2O_3 was reported to be 834.9 eV [21], La^{3+} species were dominant on the surface of $LaNi_5$. The surface atomic ratio was calculated assuming that the atomic sensitivity factors of Ni($2p_{3/2}$), La($3d_{5/2}$), and O(1s) are 13.92, 26.50, and 2.85, respectively (see Table 2) [21]. A peak at 289 eV attributed to carbonate species was recorded in the spectra for C(1s) while no peak attributed to carbide species usually at 281–283 eV was recorded (not shown).

4. Discussion

The catalytic activity of $LaNi_5$ increases gradually during the reaction at 250°C (see Fig. 1). Although crystallites of metallic nickel appear clearly after the reaction for 2 h at 250°C (see Fig. 2c), the catalytic activity at 2 h-on-stream is not so high as that at 4 or 6.5 h-on-stream. The XRD pattern for Ni_5LaO_x after the reaction also shows the presence of metallic nickel in the catalyst (see Fig. 3b), however, the catalytic activity at 250°C is not high. Hence, the formation of the metal crystallites in $LaNi_5$ does not account for the increase in the activity during the reaction at 250°C, and it shows the formation of new active sites in $LaNi_5$.

The typical structure of intermetallic compound of $LaNi_5$ is destroyed and the phase was separated into nickel metal and La^{3+} compounds during the reaction (see Fig. 2). Although no peaks attributed to nickel oxide or carbonate are present in the XRD patterns for $LaNi_5$, the result of XPS analyses shows presence of Ni^{2+} species on the surface. The binding energy of O(1s) at 529.3–529.6 eV (see Table 2) is close to that for NiO [21], suggesting

Table 2
XPS analyses for $LaNi_5$

Time-on-stream/h	Binding energy/eV (Surface composition/mol%)					Atomic ratio	
	Ni^0	Ni^{2+}	O_{Ni}	O_{La}	La($3d_{5/2}$)	O_{Ni}/Ni^{2+}	O_{La}/La
0	852.7(17.5)	855.3(12.3)	529.3(16.2)	531.7(35.4)	834.7(18.7)	1.3	1.9
0.5	852.7(15.5)	855.3(13.7)	529.3(12.8)	531.8(39.0)	834.9(19.1)	0.9	2.0
2	852.7(13.7)	855.2(14.1)	529.5(13.0)	531.8(40.9)	835.1(18.3)	0.9	2.2
4	852.7(11.0)	855.0(14.7)	529.6(12.0)	532.2(48.4)	835.5(14.0)	0.8	3.5
6.5	852.8(7.0)	854.8(19.4)	529.5(10.9)	532.2(48.0)	835.4(14.6)	0.6	3.3

presence of nickel oxide on the surface. It would be possible that nickel is oxidized in air after taken out from the reactor. However, the surface concentration of Ni^{2+} species increases with an increase in the time-on-stream and the position of the peak for Ni^{2+} shifted to a lower binding energy while the ratio of O_{Ni}/Ni^{2+} decreases (see Fig. 4, Table 2). Hence, new nickel species other than nickel oxide are believed to be formed on the surface during the reaction.

Since the catalytic activity at 250°C seems to depend on the surface concentration of Ni^{2+} (cf. Fig. 1, Table 2), we may infer that the new nickel species is the source of the increase in the activity. In the case of Ni_5LaO_x, the increase in the activity during the reaction is not so large as that of $LaNi_5$. In the former solid, $La_2O_2CO_3$ is mainly formed during the reaction and $La(OH)_3$ is not present (see Fig. 3b). On the other hand, $La(OH)_3$ and $LaCO_3OH$ are formed in $LaNi_5$ during the reaction (see Fig. 2), and it is supposed that the phase change of $LaNi_5$ is caused by water produced in the reaction. The binding energy of O(1s) for lanthanum oxide was 529.5 eV (our result), and the major peaks of O(1s) for $LaNi_5$ are at 531.7–532.2 eV. Since the binding energy of O(1s) for metal hydroxide seems to be higher than that for metal oxide [21] and the energy for lanthanum carbonate was 532.0 eV (our result), the peaks can be attributed mainly to both the hydroxyl and carbonate species. Supposing that the surface hydroxyl groups are reactive to nickel under the reaction conditions, formation of the bonding such as Ni–O–La will take place and it can account for the formation of the new nickel species on the surface. The XRD pattern of Ni_5LaO_x after the reaction shows discernible formation of $LaCO_3OH$ and it may result in the gradual increase in the catalytic activity by formation of the new nickel species. Formation of other active species such as carbide during the reaction would be possible [19,23], however, no presence of the species was evident in this study, while further investigation is necessary to clarify the details.

Acknowledgements

The authors wish to express their grateful acknowledgment to Ms. Hiroko Ban for her experimental work.

References

[1] R.S. Craig, W.E. Wallace, H. Kevin Smith, in: E.C. Subbarao, W.E. Wallace (Eds.), Science and Technology of Rare Earth Materials, Academic Press, New York, 1980.
[2] K. Soga, H. Imamura, S. Ikeda, Nippon Kagaku Kaishi 9 (1977) 1299.
[3] K. Soga, H. Imamura, S. Ikeda, Nippon Kagaku Kaishi 7 (1978) 923.
[4] K. Soga, T. Sano, H. Imamura, M. Sato, S. Ikeda, Nippon Kagaku Kaishi 7 (1978) 930.
[5] K. Soga, T. Sano, M. Sato, S. Ikeda, Nippon Kagaku Kaishi 5 (1979) 573.
[6] J.R. Johnson, Z. Gavra, P. Chyou, J.J. Reilly, J. Catal. 137 (1992) 102.
[7] A. Elattar, T. Takeshita, W.E. Wallace, R.S. Craig, Science 196 (1977) 1093.
[8] Gary B. Atkinson, Larry J. Nicks, J. Catal. 46 (1977) 417.
[9] C.A. Luengo, A.L. Cabrera, H.B. MacKay, M.B. Maple, J. Catal. 47 (1977) 1.
[10] H. Imamura, W.E. Wallace, Am. Chem. Soc., Div. Fuel Chem. 25 (1979) 82.
[11] W.E. Wallace, A. Elattar, H. Imamura, R.S. Craig, A.G. Moldovan, in: E.C. Subbarao, W.E. Wallace (Eds.), Science and Technology of Rare Earth Materials, Academic Press, New York, 1980.
[12] S. Kasaoka, E. Sasaoka, J. Misumi, Nippon Kagaku Kaishi 7 (1982) 1246.
[13] J. Barrault, D. Duprez, J. Less-Common Met. 89 (1983) 537.
[14] J. Muller, V. Pour, A. Regner, J. Catal. 11 (1968) 326.
[15] V. Pour, Collect. Czech. Chem. Commun. 35 (1970) 2203.
[16] T. Inui, M. Funabiki, M. Suehiro, T. Sezume, J. Chem. Soc., Faraday Trans. 75 (1978) 787.
[17] T. Inui, M. Funabiki, Y. Takegami, Ind. Eng. Chem. Prod. Res. Dev. 19 (1980) 385.
[18] E. Ruckenstein, Y.H. Hu, J. Catal. 161 (1996) 55.
[19] J. Barrault, A. Guilleminot, J.C. Achard, V. Paul-Boncour, A. Percheron-Guegan, L. Hilaire, M. Coulon, Appl. Catal. 22 (1986) 273.
[20] H.P. Klug, L.E. Alexander, in: X-ray Diffraction Procedures, Wiley, New York, 1954.
[21] C.D. Wagner, W.M. Riggs, L.E. Davis, J.F. Moulder, in: G.E. Muilenberg (Ed.), Handbook of X-ray Photoelectron Spectroscopy, Perkin-Elmer, MN, 1978.
[22] JCPDS powder diffraction files: 4–835(NiO); 4–850(Ni); 17–126($LaNi_5$); 24–554(La_2O_3); 26–815($LaCO_3OH$); 36–1481($La(OH)_3$); 37–804($La_2O_2CO_3$).
[23] Z.L. Wang, C. Colliex, V. Paul-Boncour, A. Percheron-Guegan, J.C. Achard, J. Barrault, J. Catal. 105 (1987) 120.